

**FLUORESCENCE PROBE STUDIES OF IONIC MICELLES IN CONCENTRATED SALT SOLUTIONS**

JIN-MING CHEN (陳錦明), TZU-MIN SU (蘇志明) and CHUNG YUAN MOU* (牟中原)

Department of Chemistry, National Taiwan University, Taipei, Taiwan, Republic of China

We have investigated the effect of salt concentration and temperature on the average aggregation number and micro-polarity of the interior of micelles of sodium dodecyl sulfate (SDS), sodium tetradecyl sulfate (STDS) and lithium dodecyl sulfate (LiDS). The transient fluorescence decay of micelle-solubilized pyrene has been measured and analyzed. An exponent weighted average aggregation number $\langle n \rangle_e$ was obtained by this technique. For SDS and STDS in NaCl solution, $\langle n \rangle_e$ increases as the temperature is lowered or salt concentration is increased; $\langle n \rangle_e$ increased from ~ 50 to ~ 250 over $[\text{NaCl}] = 0$ to 0.8 M. Due to the strong counterion binding of lithium in the micellar solution, the LiDS micelle is much smaller and does not increase appreciably even at $[\text{LiCl}] = 0.8$ M. From the fluorescence spectrum fine structure of pyrene and the fluorescence decay of the monomer and excimer, we can understand the local polarity and the water penetration to the interior of the micelle upon addition of salts and with changing temperature. The interior of the micelle becomes more nonpolar as the salt concentration is increased and the temperature is lowered. A complete kinetic analysis of the time-dependence of the fluorescence is given. The kinetic analysis is in agreement with the results reached by fluorescence spectral analysis.

INTRODUCTION

The formation of micellar aggregates in amphiphile solutions is a well-known phenomenon clearly established in early light-scattering studies¹. Usually, ionic amphiphiles form small and nearly spherical micelles at low ionic strength. When one increases the concentration of the counterion above some ionic concentration the aggregation number can increase up to 20-fold and the micelle is interpreted to undergo a sphere-to-rod shape transition. For example, when static^{2,3} and dynamic light-scattering⁴⁻⁸ techniques were used to measure the aggregation number of sodium dodecyl sulfate micelles (SDS) in NaCl solution, in the range $[\text{NaCl}] = 0 - 0.8$ M at 30°C , it was found that the aggregation number ranges from 60 to 1000; it drastically decreases at high temperature. In a previous paper⁹, we reported the use of fluorescence quenching of the micelle-solubilized fluorophore to measure an average aggregation number of the micelle. The idea is based on the increase of self-quenching of the fluorescence due to excimer formation. We concluded that the large rodlike micelle is very polydisperse and the

difference in the average aggregation size obtained by fluorescence and light-scattering studies reflects different ways of averaging. The fluorescence quenching technique measures an exponent weighted average aggregation number $\langle n \rangle_e$. In $\langle n \rangle_e$, the averaging is more heavily weighted toward smaller micelles; it is thus smaller than the weight average aggregation number that is obtained by the light-scattering technique.

For ionic micelles (cationic and anionic) in aqueous solution, the size distribution is determined by two factors¹⁰. One is the electrostatic repulsion of head groups with counterion binding on the micellar surface; the other is due to the hydrophobic interaction of the hydrocarbon chain which is related to the change of hydrogen bonding in water. When one increases the concentration of a simple salt added to the micellar solution, the effect is to decrease the electrostatic repulsion between ionic head groups. Thus the structure of the micelle (micelle size, micropolarity and microviscosity) will change, and the result is to favor micelle growth. This is reflected in a lowering of the critical micelle concentration (cmc) and a larger average micelle size.

In this paper, we use solubilized pyrene as a fluorescence probe to investigate its fluorescence behavior in aqueous micelles of sodium dodecyl sulfate (SDS), sodium tetradecyl sulfate (STDS) and lithium dodecyl sulfate (LiDS), over a range of ionic concentrations. We monitor the time-resolved fluorescence quenching due to excimer formation to obtain an exponent average aggregation number of the micelle $\langle n \rangle_e$. We investigate the change of micellar size upon the addition of salt from 0 to 0.8 M and upon the changing of the temperature from 30 to 70°C. At the same time, we use a boxcar integrator to obtain the fluorescence spectrum of pyrene. Complete kinetic analysis of the time-dependent fluorescence of monomer pyrene and the excimer gives us the rate constants for monomer decay k_1 , excimer formation k_3 , and excimer decay k_5 . From the fluorescence fine structure of pyrene and the rate constants for the fluorescence decay of the monomer and excimer, we can understand the micropolarity and water penetration into the interior region of the micelle as a function of salt concentration and temperature.

MATERIAL AND METHODS

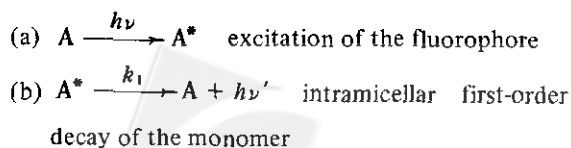
A. Reagents and Solutions. SDS (Merck A. G.) and STDS (Merck A. G.) used in this study were purified by precipitation from ethanol solution; its purity (~ 99.5%) was checked by HPLC. LiDS (Merck A. G.) was analyzed by HPLC and determined to be of higher purity than 99.5% and was used without further purification. Sodium chloride was dissolved in deionized water and chlorine was bubbled into the solution to remove any trace of bromide and iodide, since they are probable fluorescence quenchers. It was then recrystallized twice. Lithium chloride (Merck A. G.) was used without further purification. Pyrene (Riedel-Dehaen) was dissolved in benzene and the maleic acid anhydride was added and heated at 80°C to remove color impurities. The solution was

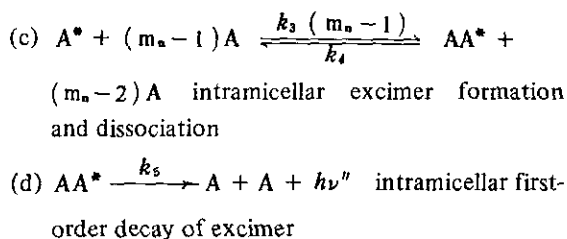
column separated through silica packing. Finally, pyrene was collected by vacuum sublimation at 160°C and 30 millitorr.

Pyrene was dissolved in n-hexane and then the n-hexane was pumped out to leave a thin layer of pyrene on the flask surface. Surfactant solution was then added to the flask and stirred at 50°C for one day to ensure complete solubilization. Oxygen was removed by a special nitrogen bubble scheme or a repeated freeze-pump and thaw operation to ensure no loss of surfactant solution.

B. Measurements. A Nd-YAG laser (Quanta-Ray DCR-2) was used to excite pyrene as 355nm. Fluorescence of wavelength 380 nm (monomer decay) and 480 nm (excimer formation and decay) were collected at 90 degrees through a 0.5 Jarell-Ash monochromator and detected by an RCA 1P28 photomultiplier. The fluorescence decay was recovered by a transient waveform recorder (Gould-Biomation 6500, 2-ns resolution) which was interfaced to a computer. The sample was kept at the desired temperature in a water thermostat to within 0.2K. In most cases, data were averaged over 300 laser shots. The fluorescence spectra of pyrene were taken by a boxcar integrator (EGG-PARC model 102-164) with gate opening time 5 μ s right after the laser firing.

C. Data Analysis. There have been many works relating the monomer fluorescence decay to the average number of fluorophores in each micelle.¹¹⁻¹³ In this paper, we follow the analysis of Atik *et al.*¹³ The kinetic scheme consists of the following processes:





Here m_n represents the occupation number of the unexcited pyrene in micelles of aggregation number n ; k_3 , k_4 and k_5 are the rate constants for excimer formation, monomer pyrene decay and excimer decay, respectively.

We assumed that (1) pyrene dissolves only in the micellar phase, (2) solubilization of pyrene is only in minor quantities (~ 1 per micelle) so that it does not change the size and structure of the micelle, (3) interchange of pyrene between micelles is slow compared to the lifetime of excited pyrene so that it does not influence fluorescence quenching, (4) $k_5 \gg k_4$ and (5) the distribution of pyrene in micelles is random, that is, the distribution of m' pyrene molecules in micelles of size n is Poissonian.

$$f_n(m') = \frac{(\bar{m}_n)^{m'} e^{-\bar{m}_n}}{m'!} \quad (1)$$

From the monomer fluorescence decay curve, we measure the fraction of unquenched first-order decay. This comes from those micelles having only one excited pyrene without any other pyrene present in it. The fraction of only one excited pyrene in micelle of size n is

$$f_n(0) = e^{-\bar{m}_n} \quad (2)$$

Given a polydisperse micelle solution with size distribution $P(n)$, the fraction of only one excited pyrene in all micelles is

$$\langle f_n(0) \rangle = \sum_n f_n(0) P(n) \quad (3)$$

For a monodisperse micelle system with average occupation number of fluorophores per micelle m .

The time dependence of the fluorescence decay of the monomer is

$$\frac{[A^*(t)]}{[A^*(0)]} = e^{m[\exp(-k_3 t) - 1] - k_4 t} \quad (4)$$

where $[A^*(t)]$ is the concentration of the excited pyrene monomer, and $[A^*(0)]$ is the initial excited monomer pyrene concentration. The detected monomer fluorescence intensity $I(t)$ is proportional to $[A^*(t)]$. The long time behavior from eq (4) is

$$I(t)/I(0) \approx e^{-k_4 t - m} \quad (5)$$

For a polydisperse micelle solution, we will have to replace the factor e^{-m} by $\langle f_n(0) \rangle$. So

$$I(t)/I(0) = \langle f_n(0) \rangle e^{-k_4 t} \quad (6)$$

Let C_p represent the stoichiometric concentration of pyrene, C represents the surfactant concentration, and cmc represents the critical micelle concentration, then we have,

$$\frac{\bar{m}_n}{n} = \frac{C_p}{C - cmc} \quad (7)$$

Then,

$$\langle f_n(0) \rangle = \sum_n e^{-n C_p / (C - cmc)} P(n) \quad (8)$$

We define an average aggregation number $\langle n \rangle_e$, which we call the exponent weighted average aggregation number, by

$$\langle f_n(0) \rangle \equiv e^{-\langle n \rangle_e C_p / (C - cmc)} \quad (9)$$

$\langle n \rangle_e$ is the exponent weighted average aggregation number reported in this study. In $\langle n \rangle_e$, the average is more heavily weighted toward the lower end. In light-scattering techniques, the average is more weighted toward the largest micelles, defined by the weight average aggregation number $\langle n \rangle_w$; therefore $\langle n \rangle_e$ is always smaller than $\langle n \rangle_w$. For a rod micelle in high salt concentration and at low temperature, the difference can be substantial⁹.

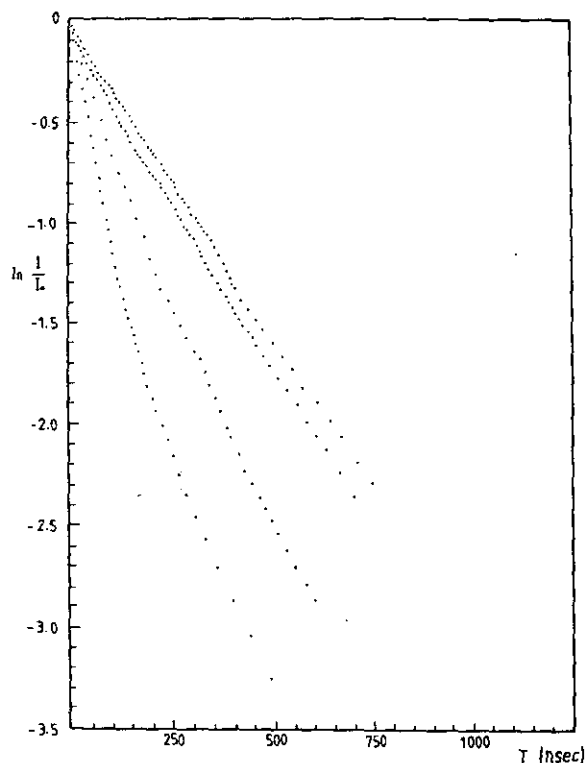


Fig. 1 Pyrene Monomer fluorescence decay : at $\lambda = 380$ nm, $[\text{SDS}] = 0.0347$ M, $[\text{NaCl}] = 0.8$ M, $T = 35^\circ\text{C}$, $[\text{pyrene}] = (\text{A}) 3 \times 10^{-5}$ M (B) 6×10^{-5} M (C) 9×10^{-5} M (D) 1.8×10^{-4} M.

RESULTS AND DISCUSSION

The fluorescence decay of excited monomer pyrene consists of two decay components: a slow exponential component corresponding to micelles having solubilized one pyrene molecule, and an initial fast nonexponential component (see Fig. 1) due to the diffusion-controlled excimer formation within micelles having solubilized two or more pyrene molecules (see eq. 4). A typical experimental result is shown in Fig. 1 for the case of SDS at $[\text{NaCl}] = 0.8$ M at several pyrene concentrations.

To make sure that no residue excimer formation exists at long time, we use the data points of approximately parallel decay (first-order) between $t = 500$ ns and $t = 1000$ ns to apply eq 6 and thus of obtain the

Table 1 Variation of the average aggregation number $\langle n \rangle_e$ of SDS, STDS and LiDS upon increasing salt concentration.

	0 M [NaCl]	0.2M [NaCl]	0.5M [NaCl]	0.8M [NaCl]
	$\langle n \rangle_e$	$\langle n \rangle_e$	$\langle n \rangle_e$	$\langle n \rangle_e$
SDS ^a	40	76	171	242
STDS ^b	50	97	162	240
LiDS ^c	< 30	~ 40	~ 45	~ 50

a. $[\text{SDS}] = 0.0347$ M, $T = 35^\circ\text{C}$

b. $[\text{STDS}] = 0.0347$ M, $T = 40^\circ\text{C}$

c. $[\text{LiDS}] = 0.0347$ M, $T = 40^\circ\text{C}$, salt is LiCl

exponent average aggregation number $\langle n \rangle_e$. We also studied the effect of varying the pyrene concentration from 3×10^{-5} to 1.8×10^{-4} M. We find that the apparent $\langle n \rangle_e$ does not change more than 10% for all the cases.

We measured the exponent weighted average aggregation number of micelles over the salt concentration range from 0 to 0.8 M, the contraction of surfactant (SDS, STDS and LiDS) is 0.0347 M. The experimental results are listed in Table 1.

From the Table 1, we can see that the micellar size increases with an increase in electrolyte concentration. For the SDS and STDS micellar systems, the micellar size increases from ~ 50 to ~ 250 over $[\text{NaCl}] = 0$ to 0.8 M. As the concentration of NaCl increases, it more effectively screens the electrostatic repulsion of the head group of the micelles and decreases the free energy. One thus observes an increase for the aggregation number of micelle. For the LiDS micellar system, the micelle size is very small. The LiDS micelle does not give much fluorescence at 480 nm and the excimer formation is too weak to evaluate a precise aggregation number. It is estimated that for $[\text{LiCl}] = 0$ M at 30°C , the aggregation number is less than 30. At a higher LiCl concentration, ($[\text{LiCl}] = 0.8$ M), the excimer yield does not increase appreciably (see next section). This behavior is due to strong counterion bonding of lithium on the micellar surface, and further addition

of salt does not change the structure of this small and tight micelle.

Since at high salt concentration, SDS can precipitate below 30°C, we measure $\langle n \rangle_e$ over the temperature range 30–70°C to avoid precipitation or secondary aggregation. The pyrene concentration is fixed at 1.8×10^{-4} M. The average aggregation numbers for various salt concentrations and temperatures are listed in Tables 5, 6 and 7. From these Tables, we observe an decrease of $\langle n \rangle_e$ as the temperature is increased; it drastically decreases at higher temperature. This is consistent with our previous results for SDS in reference 9. A thermodynamic model by Missel *et al.*⁶ has been constructed by us⁹ to explain the size change upon temperature change. Basically, at high temperature the entropy factor favors the breakup of rod micelles into smaller ones. At 70°C, the micelles are indeed small with an average aggregation number around 100 at [NaCl] = 0.5 and 0.8 M.

Micropolarity of the micellar interior: Both the fluorescence fine structure of pyrene and the kinetic rate constants of kinetic scheme (a) to (d) are sensitive to the polarity of the local environment.¹⁴⁻¹⁶ We have used these as indicators of the micropolarity of the micellar interior.

By fitting the monomer fluorescence decay curve (at 389 nm wavelength) to eq(4), we can obtain the rate constants for monomer decay k_1 and for excimer formation k_3 . The excimer fluorescence consists of two processes: a rise process due to excimer formation, the rise time of excimer formation is about 50 ns, and an excimer decay process, the lifetime of the excimer is about 100 ns. From fitting the excimer fluorescence curve (at 480 nm wavelength), we can obtain the rate constants for excimer formation k_3 and excimer decay k_5 . The resulting rate constants, obtained by varying salt concentration and temperature, are listed in Table 2 to Table 7.

A large drop of k_5 is observed when the salt

Table 2 Kinetic Data Determined from SDS Solubilized Pyrene^a

[NaCl], M	$10^6 k_1, S^{-1}$	$10^7 k_3, S^{-1}$	$10^7 k_5, S^{-1}$
0	2.4	2.8	2.2
0.2	2.6	2.5	1.8
0.5	2.9	2.2	1.4
0.8	2.5	1.2	1.1

a. [SDS] = 0.0347 M, [pyrene] = 1.8×10^{-4} M, T = 35°C

concentration is increased and temperature is lowered, that is, the lifetime of the excimer increases from ~ 50ns to ~ 150ns over 0 to 0.8 M salt concentration at T = 35°C (for STDS and LiDS, T = 40°C). This is due to the dipolar nature of the AA* excimer¹⁷. We interpret this to mean that as the size of micelle increases it repulses water molecules and the interior of the micelle becomes more nonpolar. Smaller dipolar fluctuation in the medium leads to a longer excimer lifetime.

Being a diffusion-controlled reaction, the excimer formation rate constant k_3 is dependent on the micellar size and the micro-viscosity of the micellar interior. The larger the micelle size and the higher the interior micro-viscosity the slower the excimer formation will be. From Table 2 to Table 7, we can see that the excimer formation rate constant k_3 decreases as the ionic strength is increased and the temperature is lowered. This is consistent with our

Table 3 Kinetic Data Determined from STDS Solubilized Pyrene^a

[NaCl], M	$10^6 k_1, S^{-1}$	$10^7 k_3, S^{-1}$	$10^7 k_5, S^{-1}$
0	2.6	2.5	1.7
0.2	2.8	2.1	1.4
0.5	2.8	1.8	0.9
0.8	3.0	1.6	0.7

a. [STDS] = 0.0347 M, T = 40°C

Table 4 Kinetic Data Determined from LiDS Solubilized Pyrene^a

[LiCl], M	$10^6 k_1, S^{-1}$	$10^7 k_3, S^{-1}$	$10^7 k_5, S^{-1}$
0	4.8	4.7	1.8
0.2	4.7	4.4	1.5
0.5	4.6	4.3	1.4
0.8	4.6	4.0	1.2

a. [LiDS] = 0.0347 M, T = 40°C

conclusion concerning size change. For the LiDS micellar system, the k_3 value is large compared to those for the SDS and STDS micelle systems. For the LiDS micelle system, the rise of the excimer is about 25 ns; for the SDS and STDS micelle systems, the rise time of the excimer is about 50ns. The monomer decay rate constant k_1 becomes larger the higher the temperature, although it seems to approach a constant near the high temperature limit. The excimer dissociation rate constant k_4 makes little contribution to the excimer fluorescence curve and it is much smaller than k_5 , thus we assumed $k_4 \sim 0$.⁹

We use a boxcar integrator to obtain the fluorescence spectrum of pyrene. All experiments are run at the same pyrene and surfactant concentration while the salt concentration is varied. We show here the spectra for SDS at [NaCl] = 0, 0.2, 0.5 and 0.8

Table 5 $\langle n \rangle_e$ and Kinetic Data Determined from SDS Solubilized Pyrene; [NaCl] = 0.8 M

T°C	$\langle n \rangle_e$	$10^6 k_1, S^{-1}$	$10^7 k_3, S^{-1}$	$10^7 k_5, S^{-1}$
30	270	2.3	1.0	0.9
35	242	2.5	1.2	1.1
40	206	2.6	1.3	1.4
45	181	2.8	1.4	1.8
50	158	2.7	1.6	2.5
60	118	2.7	2.0	4.0
70	95	2.8	2.3	5.0

Table 6 $\langle n \rangle_e$ and Kinetic Data Determined from SDS Solubilized Pyrene; [NaCl] = 0.5 M

T°C	$\langle n \rangle_e$	$10^6 k_1, S^{-1}$	$10^7 k_3, S^{-1}$	$10^7 k_5, S^{-1}$
30	212	2.7	2.0	1.2
35	177	2.9	2.2	1.4
40	160	3.0	2.6	1.8
45	142	3.2	2.8	2.4
50	129	3.4	2.9	3.0
60	111	3.8	3.0	5.0
70	92	4.0	3.1	6.0

M in Figures 2 and 3. The emission between 379 nm and 420 nm is that of monomer pyrene, below 420nm the emission is due to the excimer^{9,13}. It is clear from Figures 2 and 3 that excimer yield increases with increasing salt concentration. Since total amount of pyrene and surfactant are kept constant, this can only be due to the increased probability of binary encounters between pyrene molecules in the micellar phase. As the exchange of pyrene between micelles is slow (\sim microsecond) compared to fluorescence decay, one thus concludes that there is an appreciable increase of micellar size upon increasing the salt concentration. Similarly, STDS and LiDS micelles have been investigated upon addition of NaCl and LiCl. The increase in the STDS micellar size is about the same way as for SDS. The LiDS micelle is however, much smaller and does not increase appreciably even at [LiCl] = 0.8 M. The increase of excimer fluorescence is only about twofold from [LiCl] = 0 M to 0.8 M (Figure

Table 7 $\langle n \rangle_e$ and Kinetic Data Determined from SDS Solubilized Pyrene; [NaCl] = 0 M

T°C	$\langle n \rangle_e$	$10^6 k_1, S^{-1}$	$10^7 k_3, S^{-1}$	$10^7 k_5, S^{-1}$
30	44	2.3	2.3	2.0
40	41	2.6	2.9	3.0
50	35	3.3	3.5	3.6

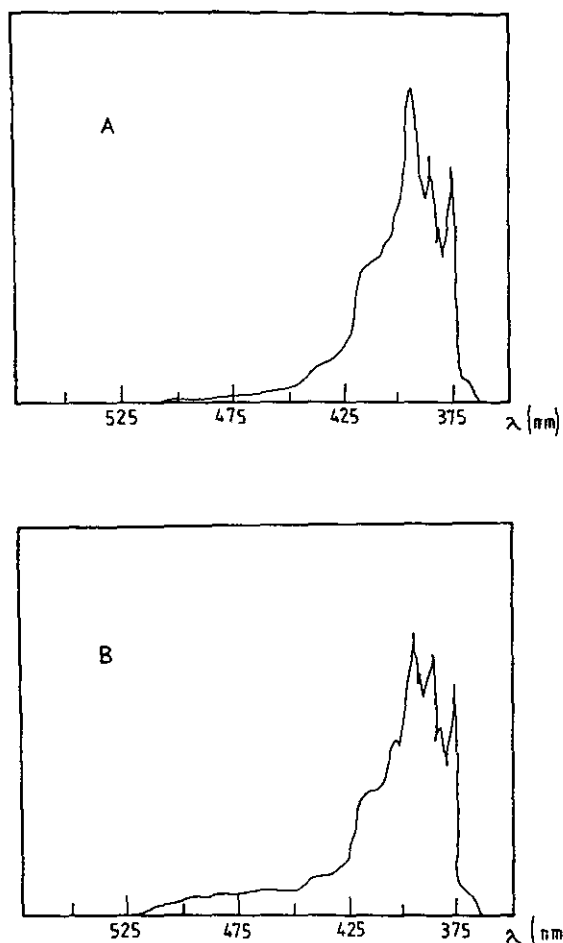


Fig. 2 Fluorescence spectra of SDS micelle solubilized pyrene, [pyrene] = 1.8×10^{-4} M, [SDS] = 0.0247 M, temperature at 35°C, (A) no salt added (B) [NaCl] = 0.2 M. Intensity in arbitrary unit.

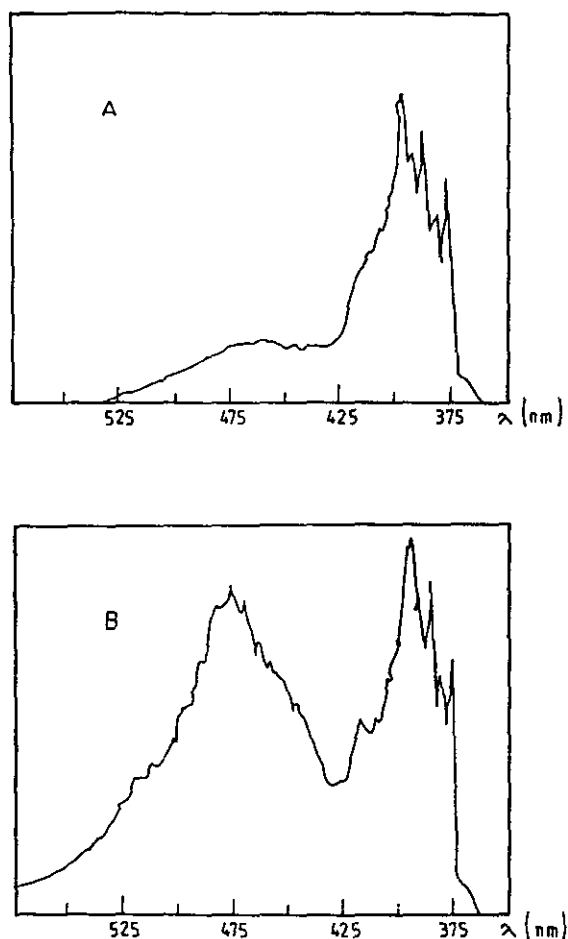


Fig. 3 Fluorescence spectra of SDS micelle solubilized pyrene, [pyrene] = 1.8×10^{-4} M, [SDS] = 0.0347 M, temperature at 35°C, (A) [NaCl] = 0.5 M (B) [NaCl] = 0.8 M. Intensity in arbitrary unit.

4).

According to Dong *et al.*¹⁸, the intensity of the first monomer fluorescence peak (375nm) I_1 , and the third fluorescence peak (396nm) I_3 is sensitively dependent on the local polarity. As the salt concentration increases and the micelle becomes larger, I_1 becomes smaller and I_3 becomes larger. Following Dong, *et al.*, we use I_1/I_3 as an indicator of the changing of micropolarity of the micellar interior upon the addition of salt and with changing tempera-

ture. The results are listed in Table 8 and Table 9. We can see that there is a gradual decrease of I_1/I_3 when the salt concentration is increased and the temperature is lowered. This indicates a gradual decrease of local polarity in the micellar interior. We interpret this to mean that the size of the micelle increases as the temperature is lowered and the ionic strength is increased. Water molecules are expelled and the interior of the micelle becomes more non-polar. This is in agreement with the conclusion

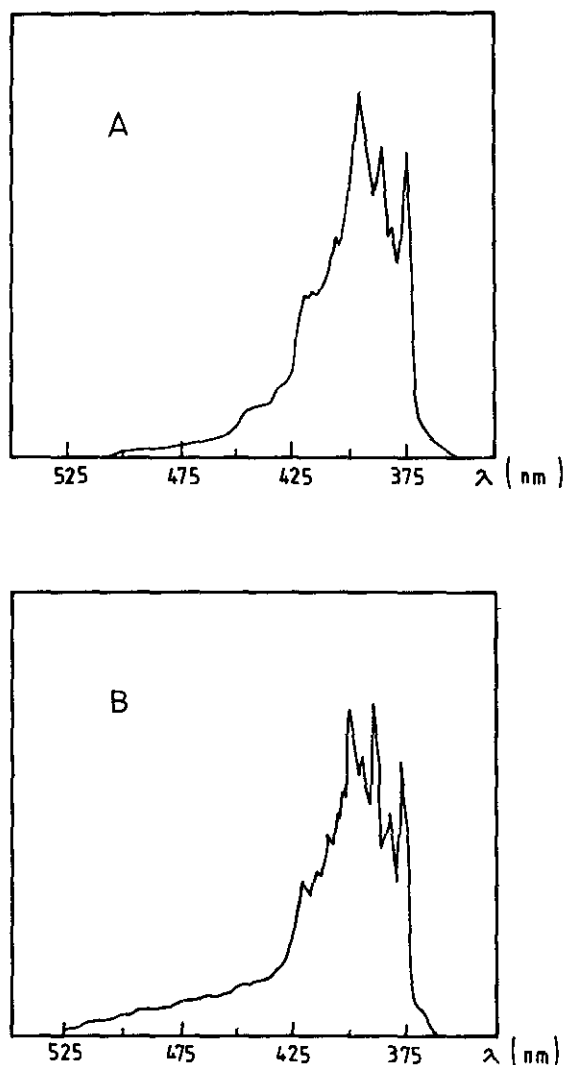


Fig. 4 Fluorescence spectra of LiDS micelle solubilized pyrene. [pyrene] = 1.8×10^{-4} M, [LiDS] = 0.0347 M, temperature at 40°C. (A) [LiDS] = 0 M (B) [LiDS] = 0.8 M.

reached by kinetic analysis. It is clear from Table 8 that the local polarity of the interior of SDS micelle is about same as STDS. Since the LiDS micelle size is much smaller, the local polarity of the interior of LiDS micelle is higher than that for SDS and STDS.

Table 8 Deoxygen Pyrene Fluorescence Spectra I_1/I_3 Value upon increasing Salt Concentration.

	0M NaCl	0.2M NaCl	0.5M NaCl	0.8M NaCl
	I_1/I_3	I_1/I_3	I_1/I_3	I_1/I_3
SDS ^a	0.96	0.88	0.86	0.81
STDS ^b	0.95	0.89	0.85	0.78
LiDS ^c	0.99	0.93	0.89	0.84

a. [SDS] = 0.0347 M, T = 35°C.

b. [STDS] = 0.0347 M, T = 40°C.

c. [LiDS] = 0.0347 M, T = 40°C, Salt is LiCl.

CONCLUSION

The problem of a large aggregation of micelles at high ionic strength has been investigated. For the case of SDS in high NaCl concentration, various techniques give similar results at low ionic strength (0.2M), but for a salt concentration above 0.3 M there are two types of results. Mysels and Princen¹, using a conventional light scattering technique, obtained a mean aggregation number of about 60 without NaCl and it increased slowly to 140 at [NaCl] = 0.5 M near the critical micelle concentration. On the other hand, a recent investigation by Ikeda et al³, indicate a large increase of m , up to 1000 at 35°C and [NaCl] = 0.8 M. So one interprets this to mean that the micelle size gradually shifts to a rodlike micelle at high salt concentration. On the other hand, Mazer et al^{5,6} used quasi-elastic light

Table 9 Deoxygen Pyrene Fluorescence Spectra I_1/I_3 Value upon increasing Temperature; [SDS] = 0.0347 M, [NaCl] = 0.8 M.

T°C	30	35	40	50	60
I_1/I_3	0.76	0.81	0.84	0.88	0.87

scattering to study the effect of NaCl on SDS micelle. They found that for SDS concentration at 0.069 M, $t = 25^\circ\text{C}$, an increase of ionic strength over 0–0.6 M resulted in an increase of the m form 80 to 1000. These results do not agree with each other. We have shown in this paper that the fluorescence technique can help us understand the polydispersity of the micelle size. Various technique gives us different values of average size due to the different ways of averaging.

We have investigated the effect of salt concentration and temperature on the average aggregation numbers of SDS, STDS and LiDS over a salt concentration range from 0 to 0.8 M and a temperature range from 30 to 70°C . We have shown that the fluorescence quenching technique can be used to study the sphere-to-rod growth of micelles in high salt concentration. The method is based on the increase of self-quenching of the fluorescence of micelle-solubilized pyrene through excimer formation. It has been shown that an exponent weighted average aggregation number $\langle n \rangle_e$ is obtained; it is smaller than weight average aggregation number obtained by quasi-elastic light-scattering technique for a polydisperse micelle system. For SDS and STDS in NaCl solution, $\langle n \rangle_e$ increases as the temperature is lowered and the salt concentration is increased; the micelle size increase from ~ 50 to ~ 250 over $[\text{NaCl}] = 0$ to 0.8 M. At high temperature, $T = 70^\circ\text{C}$, the SDS micelles are small with an average number around 100 at $[\text{NaCl}] = 0.5$ M and 0.8 M. On the other hand, LiDS micelles are small and do not change much as salts are added.

There is a good possibility that the fluorescence quenching technique can be used together with light scattering and neutron scattering to study the size distribution for the polydisperse situation and detailed thermodynamics of large micelles since they furnish a very different way of averaging the micellar size. Given recent interests in micelle thermodynamics¹⁹⁻²², we believe the fluorescence quenching technique used to obtain more experimental informa-

tion on the size distribution of micelles will be very useful. Indeed, given recent strong interests²³ in various spectroscopic probes of the self-assembly of surfactants in solution, this technique should be of more importance in the future.

From the fluorescence fine structure of pyrene and the rate constants of the fluorescence decay of monomer and excimer, we can understand the local polarity and water penetration into the interior of the micelle upon variation of salt concentration and temperature. From our experimental results, we can conclude that the local polarity of the interior of the micelle decreases upon addition of salt and with decreasing temperature. A complete kinetic analysis of the time-dependence of fluorescence has been given. The results of the kinetic analysis are in agreement with the results reached by fluorescence spectra analysis.

ACKNOWLEDGMENT

This research was supported by National Science Council of R.O.C., grant No. NSC75-0201-M002C-07.

Received October 12, 1988.

Key Word Index— Fluorescence Probe; Micellar solution; Size of Micelle; Excimer formation.

REFERENCES

1. Mysels, K. J.; Princen, L. H. *J. Phys. Chem.* **1959**, *63*, 1699.
2. Anacker, E. W. In "Solution Chemistry of Surfactants", Vol. 1, Mittal, K. L., Ed.; Plenum: New York, 1979.
3. Ikeda, S.; Hayashi, S.; Imac, T. *J. Phys. Chem.* **1981**, *85*, 106.

4. Corti, M.; Degiorgia, V. *J. Phys. Chem.* **1981**, *85*, 711.
5. Missel, P. L.; Mazer, N. A.; Benedek, G. B.; Young, C. Y.; Carey, M. C. *J. Phys. Chem.* **1980**, *84*, 1044.
6. Missel, P. L.; Mazer, N. A.; Benedek, G. B.; Carey, M. C. *J. Phys. Chem.* **1983**, *87*, 1264.
7. Flamberg, A.; Pecora, J. *J. Phys. Chem.* **1984**, *88*, 3026.
8. Mazer, N. A.; Benedek, G. B.; Carey, M. C. *J. Phys. Chem.* **1976**, *80*, 1075.
9. Chen, J. M.; Su, T.-M.; Mou, C. Y. *J. Phys. Chem.* **1986**, *90*, 2418.
10. Lindman, B.; Wennerstrom, H.; Eicke, H. F. *Topics in Current Chemistry*, Vol. 87 "Micelles" Springer-Verlag, **1980**.
11. Turro, N. J.; Yekta, A. *J. Am. Chem. Soc.* **1978**, *100*, 5951.
12. Mieler, D. J.; Klein, U. K. A.; Hauser, M. Ber. Bunsengers. *Phys. Chem.* **1980**, *84*, 1135.
13. Atik, S.; Nam, M.; Singer, L. *Chem. Phys. Lett.* **1979**, *70*, 179.
14. Kalyanasundaram, K.; Grieser, F.; Thomas, J. K. *Chem. Phys. Lett.* **1977**, *51*, 501.
15. Lianos, P.; Geozghiou, S. *Photochemistry & Photobiology* **1979**, *30*, 355.
16. Nakajima, A. *Spectrochim.* **1973**, *30A*, 860.
17. Turro, N. J. "Modern Molecular Photochemistry", **1979**.
18. Dong, D. C.; Winnik, M. A. *Photochemistry & Photobiology* **1982**, *35*, 17.
19. Stcker, M.M.; Benedek, G. B. *J. Phys. Chem.* **1984**, *88*, 6519.
20. Eriksson, J. C.; Ljunggren, S.; Hendriksson, U. *J. Chem. Soc. Faraday Trans. 2*, **1985**, *81*, 833.
21. McMullen IV, W. E.; Gelbart, W. M.; Ben-Shaul, A. *J. Phys. Chem.* **1984**, *88*, 6649.
22. Hsieh, T-K; Master Thesis, National Taiwan University, **1986**.
23. Grieser, F. Drummond, C. Y., *J. Phys. Chem.* **1988**, *92*, 5580.

